Fluids and Barriers of the CNS

RESEARCH

Open Access

Glucagon-like peptide-1 receptor modulates cerebrospinal fluid secretion and intracranial pressure in rats

Mette N. Jensen[1], Ida M. E. Israelsen[1], Jonathan H. Wardman[1], Dennis B. Jensen[1], Daniel B. Andersen[2], Trine L. Toft-Bertelsen[1], Martin F. Rath[1], Jens Juul Holst[2], Mette M. Rosenkilde[2] and Nanna MacAulay[1*]

Abstract

Background Cerebrospinal fluid (CSF) is produced and absorbed at a balanced rate to maintain a constant intracranial pressure (ICP). The CSF dynamics are, however, disturbed in several pathological conditions, leading to elevated ICP, which may have fatal outcomes if left untreated. Treatment options for these conditions are limited to invasive neurosurgery, and novel pharmacological approaches to manage ICP in pathology are sought. Here, we aimed to demonstrate the potential of the glucagon-like peptide-1 receptor (GLP-1R) as such a target.

Methods We administered male rats with intraperitoneal (i.p.) or intracerebroventricular (i.c.v.) GLP-1R agonist (exendin-4) or antagonist (exendin-9-39) followed by in vivo determination of CSF dynamics. GLP-1R expression in the CSF-secreting choroid plexus was demonstrated with RNAScope in situ hybridization and western blotting and transporter activity with radio-isotope flux assays.

Results GLP-1R activation increased the CSF secretion rate with an associated elevation of the ICP, whereas inhibition of the receptor reduced the rate of CSF secretion. These effects were observed with central, but not peripheral, administration of the agonist and antagonist, suggesting receptor expression on the luminal, CSF-facing side of the choroid plexus, which aligned with GLP-1R-mediated modulation of luminally-expressed transporters in excised choroid plexus. Low level GLP-1R expression was demonstrated in the choroid plexus at mRNA and protein levels.

Conclusion Modulation of GLP-1R affects CSF production, which suggests that GLP-1R-mediated signalling may have the potential to control ICP in pathological conditions with disturbed CSF homeostasis.

Keywords GLP-1, ICP, CSF, Choroid plexus, Hydrocephalus, IIH

*Correspondence:
Nanna MacAulay
macaulay@sund.ku.dk
[1]Department of Neuroscience, Faculty of Health and Medical Sciences, University of Copenhagen, Blegdamsvej 3, Copenhagen N DK-2200, Denmark
[2]Department of Biomedical Sciences, Faculty of Health and Medical Sciences, University of Copenhagen, Copenhagen, Denmark

Introduction

The mammalian brain is bathed in the cerebrospinal fluid (CSF) that is continuously produced by a specialized tissue, the choroid plexus. This tissue is located in the brain ventricles, which are fluid-filled cavities inside the brain. Approximately 500 ml of fluid is secreted in the adult human brain each day and circulates through the four ventricles to the subarachnoid space prior to reabsorption [1].

A range of cerebral pathologies, such as traumatic brain injury, ischemic stroke, and hydrocephalus, associate with dysregulation of the brain fluid homeostasis, leading to debilitating, or even fatal, brain water accumulation and ensuing elevation of the intracranial pressure (ICP). These conditions are presently treated by neurosurgical implantation of a ventriculo-peritoneal shunt, by which excess fluid is diverted from the brain ventricles into the peritoneal cavity [2], or – in severe cases of brain edema - craniectomy, by which temporary removal of a portion of the skull relieves the pressure on the brain tissue [3]. The current treatment of elevated ICP is thus essentially limited to invasive surgical methodology based on hydro-mechanical principles and is associated with many complications. To develop future therapeutic approaches aimed at controlling pathological brain fluid accumulation, it would be expedient to modulate the rate of CSF secretion pharmacologically.

Glucagon-like peptide-1 (GLP-1) was originally discovered as a gut hormone with various gastrointestinal functions, i.e., gastric acid secretion and gastric emptying [4, 5]. It was later demonstrated to promote food satiety and weight loss [6–8], possibly via intracerebral actions of GLP-1 [9–11]. Importantly, GLP-1 appears to modulate systemic fluid homeostasis via its action on epithelia such as the renal proximal tubuli and the intestine [10, 12–14]. It acts via the G protein-coupled receptor, GLP-1R, that is expressed throughout the body, i.e., detected in pancreas, lung, heart, kidney, stomach, and intestine, as well as in multiple regions and cell types of the brain [15]. GLP-1R is involved in a vast range of physiological functions and appears as a potential pharmacological target for a range of pathologies, including those of a metabolic origin, cardiovascular conditions, and dementia [16–19].

We recently demonstrated *Glp1r* transcript in the rat choroid plexus [20], which aligns with an initial suggestion of its presence at the protein level [21]. The latter study, in addition, indicated the ability of a GLP-1R agonist to modulate the ICP in a rat model of hydrocephalus, suggesting that GLP-1 could serve as a potential regulator of CSF secretion via its action on the GLP-1R expressed in the CSF-secreting choroid plexus. We here set out to determine the modulatory effect of a GLP-1R agonist and an antagonist on the rate of CSF secretion and the ICP in rats by in vivo experimentation, and to resolve the underlying molecular pathways in excised choroid plexus.

Methods

Experimental animals

Nine-week-old male Sprague Dawley rats (Janvier labs) and eight-month-old male *Glp1r*-tdTomato reporter mice [22] were used for the study. The animals were housed in a temperature-controlled room with a 12 h:12 h light-dark cycle and had free access to a standard rodent pellet diet and tap water prior to experiments. The animal experiments conformed to the legislations for animal protection and care in the European Community Council Directive (2010/63/EU) and were approved by the Danish Animal Experiments Inspectorate (License no. 2018-15-0201-01595 and 2018-15-0201-01397).

Anaesthesia and physiological parameters

Prior to in vivo experimentation, the animals were anesthetised with intraperitoneal (i.p.) injections of 6 mg/ml xylazine followed 5 min later by 60 mg/ml ketamine (ScanVet) in sterile water (0.17 ml/100 g bodyweight). Body temperature was maintained at 37 °C by a homeothermic monitoring system (Harvard Apparatus). To sustain anaesthesia in experiments lasting longer than 30 min, the animals were re-administered with half a dose of ketamine based on foot reflex. Where the anaesthesia exceeded 30 min (ICP monitoring and ventriculo-cisternal perfusion), surgical tracheotomy and mechanical ventilation were employed using the VentElite system (Harvard Apparatus) to ensure stable respiratory partial pressure of carbon dioxide (pCO_2) and arterial oxygen saturation, and thus stable plasma pH and electrolyte content. The mechanical ventilation was adjusted for inhalation of 0.9 l/min humidified air mixed with 0.1 l/min O_2 with approximately 2.6 ml/breath, 80 breath/min, a positive end-expiratory pressure (PEEP) at 2 cm, and 10% sigh for a 350 g rat. The ventilation was adjusted according to the exhaled end-tidal CO_2 ($etCO_2$) measured with a capnograph (Type 340, Harvard Apparatus) and a pulse oximeter (MouseOx® Plus, Starr Life Sciences), aiming for a 5.0 ± 0.5 kPa blood pCO_2 and arterial oxygen saturation of 98.8–99.4% before administration of control or drug solutions.

Solutions and chemicals

The majority of in vivo experiments were conducted with heated (37 ° C) and gas-equilibrated CO_2/HCO_3^--buffered artificial cerebrospinal fluid (HCO_3^--aCSF, see Table 1 for concentrations). In experiments where the solution could not be gas-equilibrated (e.g., isotope influx/efflux experiments and in the ICP pressure probe), aCSF was buffered with HEPES (HEPES-aCSF, see Table 1 for concentrations).

Table 1 aCSF concentrations

Chemical	HCO_3^--aCSF	HEPES-aCSF
NaCl (mM)	120	120
KCl (mM)	2.5	2.5
$CaCl_2$ (mM)	2.5	2.5
$MgSO_4$ (mM)	1.3	1.3
NaH_2PO_4 (mM)	1	1
Glucose (mM)	10	10
$NaHCO_3$ (mM)	25	
Na-HEPES (mM)		17
pH	7.4 (with 95% O_2/5% CO_2)	7.4 (with NaOH)

Stock solutions of Exendin-4 (Ex4; 10 mM in dH_2O; ApexBio) and Exendin-9-39 (Ex9-39; 1 mM in dH_2O; ThermoFisher and Tocris) were aliquoted and stored at -80 °C until use. Ex4 was used at a concentration of 0.2 µg/kg for systemic (i.p.) delivery, which was demonstrated to promote a physiological effect in in vivo experiments and human patients [23–28], whereas Ex9-39 was employed at much higher concentration (128 µg/kg [29, 30], due to its competitive antagonism).

ICP measurements in anaesthetized rats

Anaesthetized and ventilated rats were placed in a stereotactic frame, had the skull exposed, and a cranial window of 3.6 mm in diameter was drilled (coordinates: 4 mm posterior to bregma, 1 mm lateral to the midline) with care not to damage the dura. The epidural probe (PlasticsOne, C313G) was secured with dental resin cement (Panavia SA Cement, Kuraray Noritake Dental Inc.) above the dura. The ICP cannula filled with HEPES-aCSF was connected to a pressure transducer (APT300) and transducer amplifier module TAM-A (Hugo Sachs Elektronik). To ensure a continuous fluid column between the dura and the epidural probe, approximately 5 µl HEPES-aCSF was injected through the epidural probe. The ICP signal was visualized and recorded at 1 kHz sampling rate using BDAS Basic Data Acquisition Software (Harvard Apparatus, Hugo Sachs Elektronik). Jugular compression was applied to confirm proper ICP recording. During intracerebroventricular (i.c.v.) delivery of Ex4 and Ex9-39, a 0.5 mm burr hole was drilled on the contralateral side of the skull (1.3 mm posterior, 1.8 mm lateral to bregma), and a 4 mm brain infusion cannula (Brain infusion kit2, Alzet) was placed into the lateral ventricle. When the ICP signal stabilized, 37 °C HCO_3^--aCSF containing dH_2O (vehicle) was slowly infused (0.5 µl/min) with a peristaltic pump for 25 min prior to solution shift to either control solution (HCO_3^- -aCSF-dH_2O), Ex4 (HCO_3^--aCSF + 9 µM Ex4 in dH_2O) or Ex9-39 (HCO_3^--aCSF + 90 µM Ex9-39 in dH_2O).

Live imaging of CSF movement

Anaesthetized rats were placed in a stereotactic frame and a burr hole in the skull (same coordinates as for ICP) was made. A Hamilton syringe (RN 0.40, G27, a20, Agntho's) was inserted 4 mm deep into the lateral ventricle. 15 µl HCO_3^--aCSF containing either vehicle (dH_2O), Ex4 (0.1 µM) or Ex9-39 (1 µM) was delivered i.c.v. (1.5 µl/s). This first injection was intended to allow the inhibitors to act on their target transporters prior to the introduction of the fluorescent dye 5 min later, where the procedure was repeated with the inclusion of carboxylate dye (10 µM; MW = 1091 kDa; IRDye 800Cw, P/N 929–08972, LI-COR Biosciences). For i.p. injections, vehicle (dH_2O), Ex4 (0.2 µg/kg) or Ex9-39 (128 µg/kg) was injected 29 min prior to injection of the carboxylate dye. For both i.c.v. and i.p. drug delivery, image acquisition at 30 s intervals was initiated 1 min after dye injection (800 nm channel; 85 µm resolution; for 10 min) using a Pearl Trilogy Small Animal Imaging system (LI-COR Biosciences). To secure a stable head position, the rat was placed in a customized tooth holder. A white field image was acquired at the termination of each experiment prior to verification of proper targeting of the ventricular compartment. The region of interest (ROI) for fluorescent signal determination posterior from lambda was determined based on the white field image. The fluorescent intensity was normalized to the initial fluorescent intensity in the first image captured 30 s after the rat was positioned in the scanner. The data were analyzed using LI-COR Image Studio 5.2 (LI-COR Biosciences).

Brain water quantification

Brain water content was determined following both i.c.v. and i.p. injections of the test solutions. For i.c.v. injections, two injections of 15 µl vehicle (dH_2O), Ex4 (0.1 µM), or Ex9-39 (1 µM) were performed 24 h and 16 h prior to brain water determination. For i.p. injections, brain water was determined after injecting 1 ml/kg of either vehicle (dH_2O) or Ex4 (2 µg/kg) at 24 h, 16 h, and 30 min prior to weighing the brain. The brain was swiftly (∼ 1 min) isolated from anaesthetized and decapitated rats. The isolated brains were placed into a pre-weighed porcelain beaker (Witeg) and weighed immediately thereafter (wet brain weight). The brains were left in the oven to dry at 100 °C for 3 days. Subsequently, the brains were weighed again (dry brain weight). The brain water content was calculated from the evaporated water weight and expressed as percentage brain water.

Measurement of cAMP production mediated by activation of rat GLP-1R

Cells were transiently transfected with cDNA encoding the rGLP-1R, and the cAMP quantification was done with an enzyme fragment complementation (EFC)-based

assay [31]. In brief, COS-7 cells (ATCC, CRL-1651 for Ex4) and HEK293 cells (ATCC, CRL-1573 for Ex9-39) were grown in Dulbecco's modified Eagle's medium (DMEM) 1885 supplemented with 10% foetal bovine serum (FBS), 2 mM glutamine, 180 units/ml penicillin, and 45 g/ml streptomycin at 10% CO_2 and 37 °C. One day after seeding in culture flasks (6 mio cells/flask), cells were transiently transfected with 40 µg receptor DNA using the calcium phosphate precipitation method [32]. One day after transfection, the cells were seeded in white 96-well plates at a density of 3.5×10^4 cells per well. The following day, the cells were washed twice with HEPES-buffered saline (HBS) and incubated with HBS containing 1 mM 3-isobutyl-1-methylxanthine (IBMX) for 30 min at 37 °C. To determine agonistic activity, Ex4 was added in increasing concentrations (0.1 pM to 10 nM), and incubated for 30 min at 37 °C. To determine the antagonistic properties of Ex9-39, the cells were pre-incubated for 10 min with increasing concentrations of Ex9-39 (1 nM to 1 µM) followed by the addition of 100 pM GLP-1, corresponding to 50% of maximal activity, and incubated for an additional 20 min. The HitHunterTM cAMP XS assay (DiscoverX, Herlev, Denmark) was carried out in duplicates according to the manufacturer's instructions. The dose-response curves were generated by non-linear regression analyses with constant Hill coefficient in the GraphPad Prism v. 9 program (GraphPad Software).

RNAscope in situ hybridisation

Rats were euthanized, the brains isolated and quickly frozen on dry ice (5 min) prior to storage at -80 °C for up to one week before experiments. Twelve µm cryostat sections of the brains were prepared, allowing visualization of the choroid plexuses of the lateral and fourth ventricles, and treated according to the manufacturer's protocol for freshly frozen sections (ACDBio; #320513). The sections were subsequently employed for RNAscope using the RNAscope Fluorescent Multiplex Reagent Kit (ACDBio; #320850), according to manufacturer's protocol (ACDBio; #320293). The probes detected *Glp1r* transcripts (targeting 292–1166 on NM_012728.1) and *Atp1a1* (targeting 308–1681 on NM_012504.1) and the signal was visualised with an Axioplan 2 epifluorescence microscope with 40x/0.75 Plan-Neofluar and 5x/0.16 EC Plan-Neofluar objectives and an Axiocam 702 digital camera (Zeiss).

Western blot

Choroid plexuses from the lateral and fourth ventricle (and hypothalamus) were isolated and stored at -80 °C until homogenization in 25 (200 for hypothalamus) µl RIPA buffer (in mM: 150 NaCl, 50 Tris pH 8.0, 5 EDTA and 0.5% sodium deoxycholate, 0.1% SDS and 1% Triton X-100) containing proteinase inhibitors (0.4 mM pefabloc and 8 µM leupeptin, Sigma-Aldrich) before sonication (thrice, 70% power, 10 s, Sonoplus, Bandelin) on ice. The lysed tissue was centrifuged (13000 rpm, 3 min, 4 °C) and the supernatant was transferred to a clean Eppendorf tube (low-bind protein) prior to protein concentration determination with the DC Protein Assay (Bio-Rad) according to manufacturer's instruction. 20 µg protein was loaded on precast SDS-PAGE gels (4–20% Criterion TGX, Bio-Rad) and immobilon-FL membranes (Merck Milipore) employed for the transfer. Primary and secondary antibodies were diluted 1:1 in Odyssey blocking buffer (LI-COR): PBS-T. Primary antibodies anti-GAPDH (AB2302, Milipore; 1:800) and anti-GLP-1R (EPR21819, Abcam; 1:1000), and secondary antibodies IRDye 680RD donkey anti-chicken (LI-COR, P/N 925-68075; 1:10000:) and IRDye 800CW goat anti-rabbit (LI-COR, P/N 926-32211, 1:10000:) were employed. Images were obtained by the Odyssey CLx imaging system and analyzed by Image studio v. 5.2 (LI-COR bioscience).

Fluorescent imaging reporter mice

The *Glp1r*-tdTomato reporter mice that express the reporter protein, tdTomato, in GLP-1R-expressing cells [22] were anaesthetized prior to transcardial perfusion with 0.9% NaCl followed by perfusion fixation with 4% paraformaldehyde (PFA) in phosphate buffer. The brains were isolated, placed in 4% PFA for 24 h, and transferred to a 30% sucrose solution (in phosphate-buffered saline) overnight prior to quick-freezing on dry ice, and storage at -20 °C. The brains were sliced in 12 µm sections using a cryostat 500 (Leica CM3050 S) allowing visualization of the choroid plexuses in the lateral and fourth ventricles. Visualization of the tdTomato fluorescence was performed as described above.

CSF production rate

The ventriculo-cisternal perfusion was performed using an infusion cannula (Brain infusion kit 2, Alzet) stereotaxically placed in the right lateral ventricle of an anesthetized and ventilated rat (using the same coordinates as for ICP), through which a pre-heated (37 °C, SF-28, Warner Instruments) dextran-containing solution (HCO_3^--aCSF containing 1 mg/ml TRITC-dextran (tetramethylrhodamine isothiocyanate-dextran, MW = 155 kDa; T1287, Sigma)) was perfused at 9 µl/min. CSF was sampled at 5 min intervals from a cisterna magna puncture. The cisterna magna puncture and associated continuous fluid sampling prevent elevation of the ICP during the procedure. The dilution of the infused solution is attributed to endogenously secreted CSF, irrespective of the origin of this fluid. After 60 min of perfusion, the control aCSF was replaced with one containing either vehicle or the protein kinase A (PKA) inhibitor H89 (Sigma-Aldrich, 250 µM). The fluorescence of the cisternal collections

was measured in a microplate photometer (545 nm, Synergy™ Neo2 Multi-mode Microplate Reader; BioTek Instruments), and the production rate of CSF was calculated from the equation:

$$V_p = r_i * \frac{C_i - C_o}{C_o}$$

Where V_p = CSF production rate (µl/min), r_i = infusion rate (µl/min), C_i = fluorescence of inflow solution, C_o = fluorescence of outflow solution, calculated based on stable time intervals from 60-80 min and 110–130 min from initiation of the experimental procedure.

Radioisotope flux assays

Isolated rat brains were kept in cold HEPES-aCSF (4 °C, pH 7.4) for ~10 min prior to isolation of the lateral choroid plexuses. Subsequently, the choroid plexuses were transferred to warm HEPES-aCSF (37 °C, pH 7.4) for a 10 min recovery period before initiation of the flux assay. For influx of $^{86}Rb^+$ (K^+ congener), the tissue was placed in 37 °C HEPES-aCSF containing 1 µCi/ml $^{86}Rb^+$ (022-105721-00321-0001, POLATOM) and 4 µCi/ml ^{3}H-mannitol (NET101, Perkin Elmer; extracellular marker) for 2 min [33] with and without 2 mM ouabain (in aCSF; O3125, Sigma; Na^+/K^+-ATPase inhibitor), and with and without 0.1 µM Ex4 or 1 µM Ex9-39 (randomly assigned). After isotope accumulation, the choroid plexuses were rinsed in ice-cold isotope-free HEPES-aCSF containing 2 mM ouabain, 20 µM bumetanide (Sigma, B3023; inhibitor of Na^+,K^+,$2Cl^-$ cotransporter, NKCC1), and 100 µM $BaCl_2$ (K^+ channel inhibitor) preventing efflux of intracellular $^{86}Rb^+$ during washing, and placed in scintillation vials containing 200 µl Solvable (6NE9100, Perkin Elmer). For efflux of $^{86}Rb^+$, the choroid plexuses were placed in 37 °C HEPES-aCSF containing 1 µCi/ml $^{86}Rb^+$ and 4 µCi/ml ^{3}H-mannitol for 10 min allowing isotope accumulation into the tissue. The choroid plexuses were randomly assigned to aCSF containing either 50 µM H89 or vehicle (dH_2O) or to a condition with or without 20 µM bumetanide or vehicle (0.1% DMSO) and with or without, Ex4 (0.1 µM) or Ex9-39 (1 µM). Afterward, the choroid plexuses were rinsed quickly in 37 °C isotope-free HEPES-aCSF and transferred to new wells containing 37 °C isotope-free HEPES-aCSF containing the predetermined condition at 10 s intervals to obtain the $^{86}Rb^+$ efflux rate constant. The choroid plexuses were transferred to scintillation vials containing 200 µl Solvable, and the efflux medium from each well was transferred to separate scintillation vials. After the choroid plexuses had dissolved (>4 h), 2 ml Ultima Gold™ XR scintillation liquid (6013119, Perkin Elmer) was added to each scintillation vial, and the isotope content was determined using a Tri-Carb 2900TR Liquid Scintillation Analyzer (Packard). ^{3}H-mannitol counts were used to correct for the extracellular background of $^{86}Rb^+$. For efflux data, the natural logarithm of the $^{86}Rb^+$ counts at each time point (A_t) was normalized to the initial $^{86}Rb^+$ count (A_0) and presented as a function of time. Linear regression on the data revealed the $^{86}Rb^+$ efflux rate constant.

Statistics

All data are presented as mean ± SEM. Statistical tests were performed using GraphPad Prism v. 9 (GraphPad Software), and a p-value < 0.05 was considered statistically significant. Student's unpaired t-test and one-way ANOVA with multiple comparisons were used for statistical analyses as indicated in the figure legends and outliers identified with Grubb's test (as indicated in figure legends).

Results

Peripheral administration of GLP-1R analogues does not affect CSF dynamics in rats

To determine whether the reported GLP-1-mediated modulation of ICP [21] originated in altered CSF secretion, we employed the synthetic agonist exendin-4 (Ex4) which has longer systemic half-live than GLP-1, due to insensitivity to the protease dipeptidyl peptidase 4 [34, 35] and the synthetic antagonist exendin-9-39 (Ex9-39). To validate their efficiency on the rat GLP-1R, we employed cell lines transfected with the cDNA encoding the receptor (see Methods for details). Upon measurements of cAMP accumulation as a readout of G_s activation, Ex4 acted as a potent agonist on rGLP-1R with an EC_{50} of 102 pM (log EC_{50}; -9.99 ± -0.14, $n = 6$, Fig. 1A). Ex9-39 inhibited GLP-1-induced cAMP accumulation via the rGLP-1R with an inhibitory potency of 84,5 nM (log IC_{50}; -7.07 ± -0.24, $n = 3$, Fig. 1A). The two GLP-1R ligands were delivered i.p. 30 min prior to the determination of the CSF flow by live imaging of a fluorescent dye delivered to the lateral ventricle, with the rostro-caudal dispersion rate of the fluorescent dye serving as a proxy for the CSF secretion rate [36, 37]. Quantification of the rate of dye flow was determined by its entry into the region of interest (ROI, indicated with a yellow box in Fig. 1B, left panel); lateral ventricle targeting was verified postmortem (Fig. 1B, right panel). Figure 1C illustrates representative images of CSF dye flow in a control (dH_2O-treated) rat. Quantification of the dye flow demonstrated that the CSF flow rate was undisturbed by peripheral administration of Ex4 (0.14 ± 0.01 a.u./min, $n = 7$ vs. 0.11 ± 0.01 a.u./min in the control rats, $n = 8$, $p = 0.13$) and Ex9-39 (0.12 ± 0.01 a.u./min, $n = 7$, $p = 0.95$, Fig. 1D-E). Prolonged exposure to peripheral Ex4 administration (24 h, 16 h, and 30 min prior to termination) did not increase the overall brain water content (78.6 ± 0.1% water in Ex4-treated rats versus their vehicle (dH_2O)-treated control

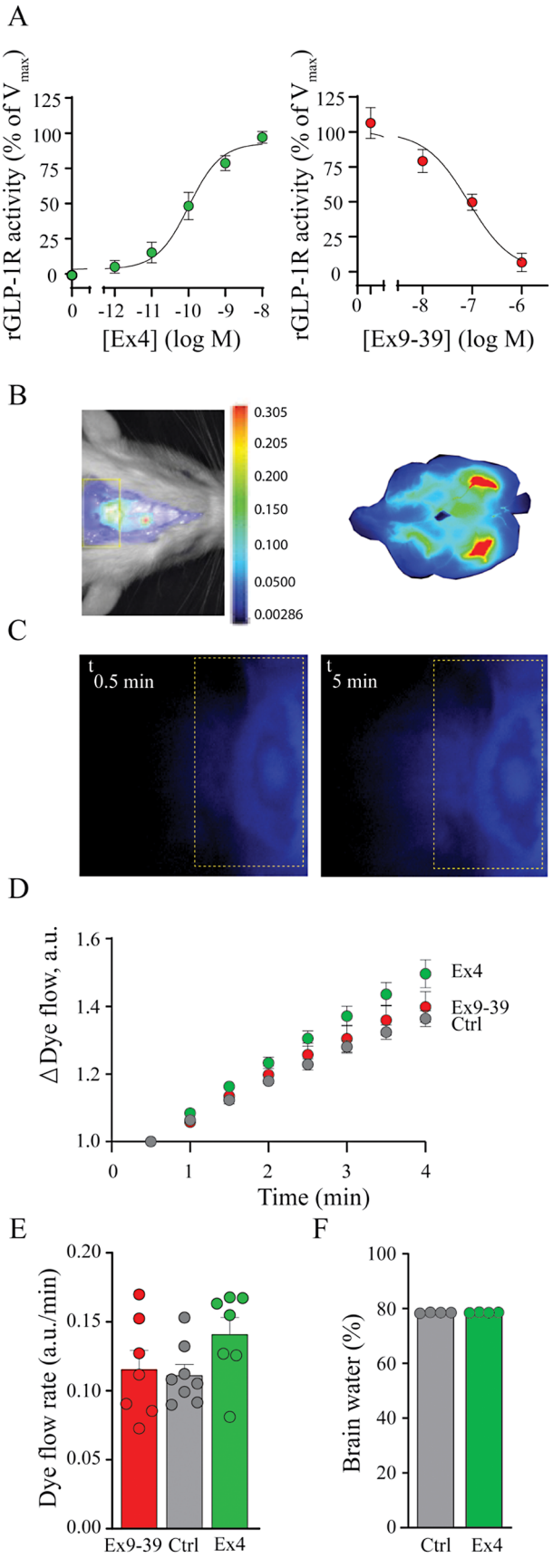

Fig. 1 CSF flow is undisturbed with peripheral delivery of GLP-1R agonist and antagonist. **A** Effect of Ex4 (left panel, $n=6$) and Ex9-39 (right panel, $n=3$, quantified in the presence of 100 pM GLP-1) on cAMP accumulation mediated by the rGLP-1R expressed in transiently transfected cells (COS7 cells for Ex4 and HEK293 cells for Ex9-39). **B** Rat brain after i.c.v. carboxylate dye injection with superimposed pseudo-color. The yellow box indicates ROI starting from lambda (left panel), and demonstration of correct targeting to the ventricular system (right panel). **C** Representative images of dye flow in a control rat (30 min post-vehicle i.p. injection) obtained at t = 0.5 s and t = 5 min, with the ROI indicated in a yellow box (same orientation of all images in **B** and **C**). **D** The dye intensity normalized to that obtained in the first image is plotted as a function of time, representing flow rate, $n=7$–8. **E** Quantification of the dye intensity (flow rate) determined from linear regression of data in (**C**) over the 4 min time window (with one outlier removed from the control group). **F** Brain water content in rats following i.p. delivery of Ex4 or vehicle 24 h, 16 h, and 30 min prior to weighing the brains ($n=4$). Results are shown as mean ± SEM and statistical significance was evaluated with one-way ANOVA followed by Dunnett's *post-hoc* test (**E**) and Student's unpaired t-test (**F**). Non significance is not shown for clarity

counterparts with 78.5 ± 0.1% water, $n=4$, $p=0.4$, Fig. 1F). These results demonstrate that peripheral administration of Ex4 or Ex9-39 does not modulate the CSF dynamics under the tested experimental conditions.

Central administration of GLP-1 receptor analogues alters CSF flow

Considering the abundant systemic targets for peripherally delivered GLP-1R modulators [12, 38–40], which could affect brain fluid dynamics indirectly, we determined the effect of delivering the GLP-1R analogues into the lateral ventricle prior to quantification of the CSF flow. The GLP-1R agonist Ex-4 increased the rate of CSF flow by ~38% (0.18 ± 0.01 a.u./min, $n=6$ vs. 0.13 ± 0.01 a.u./min in control rats, $n=6$, $p<0.05$, Fig. 2A-B). I.c.v. administration of Ex9-39 significantly reduced the rate of CSF flow by ~60% (0.05 ± 0.01 a.u./min, $n=6$) compared to the control rats ($p<0.001$, Fig. 2A-B). Determination of brain water content after i.c.v. administration of the analogues 24 h and 16 h before the brain excision demonstrated no prolonged change in overall brain water content upon this GLP-1R analogue treatment (78.6 ± 0.1%, $n=5$ in control rats vs. 78.7 ± 0.1%, $n=4$ in Ex4-treated rats, $p=0.97$ and 78.7 ± 0.2%, $n=4$ in Ex9-39-treated rats, $n=4$, $p=1$, Fig. 2C). These results suggest that central modulation of GLP-1R activity alters CSF secretion, but these acute effects are not of sufficient magnitude or duration to establish prolonged changes in overall brain water content.

GLP-1R-mediated increase in CSF secretion increases ICP

To determine if GLP-1R-mediated changes in CSF secretion could modulate ICP, we quantified the ICP in rats during slow (0.5 µl/min) i.c.v. infusion of Ex4, Ex9-39, or vehicle (control). The baseline ICP (obtained prior to infusion of the agonist and antagonist) across all

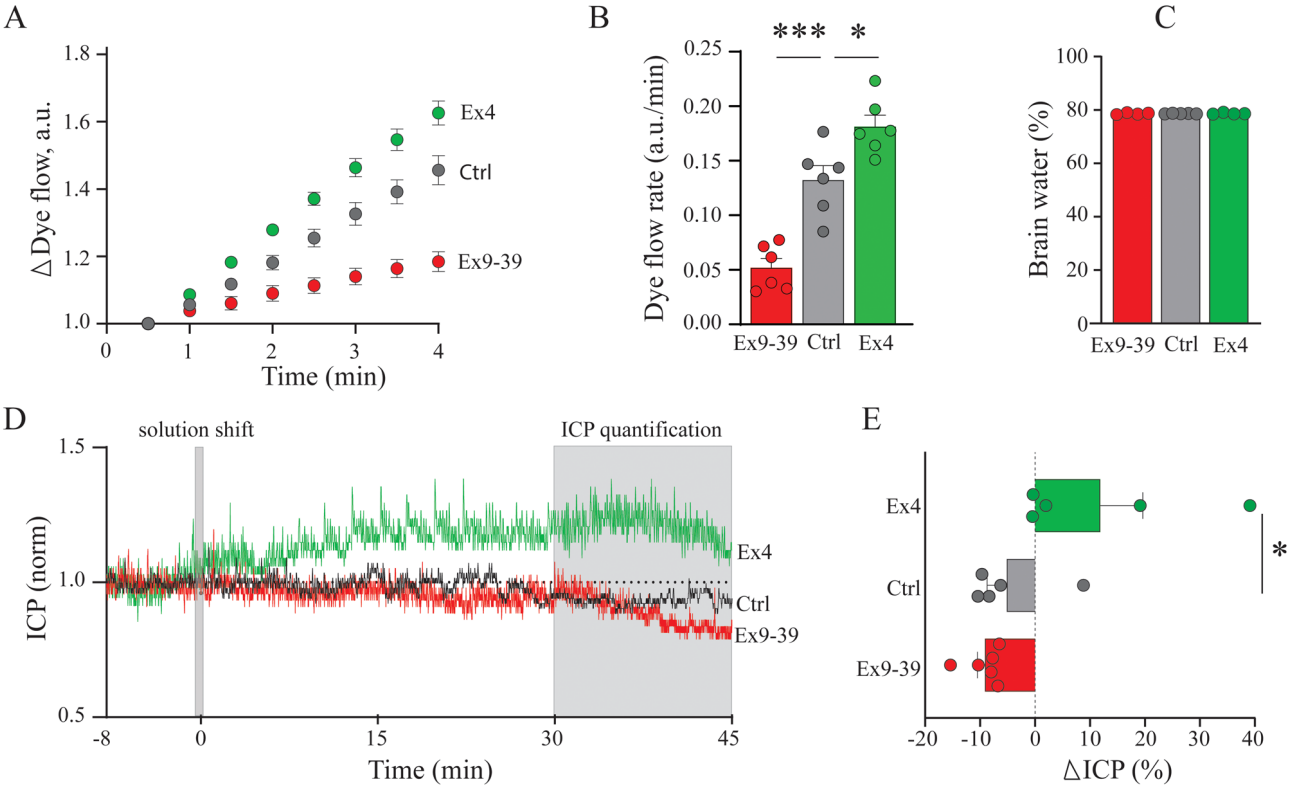

Fig. 2 Central administration of GLP-1R modulators alters CSF flow and ICP. **A** Dye flow in Ex9-39-, vehicle-, or Ex4-treated rats post-i.c.v. injection with the dye intensity normalized to that obtained in the first image is plotted as a function of time, representing flow rate, $n = 6$. **B** Quantification of the dye intensity (flow rate) determined from linear regression of data in (**A**) over the 4 min time window. **C** Brain water content in rats following i.c.v. delivery of Ex4 or vehicle 24 h and 16 h prior to weighing the brains ($n = 4–5$). **D** Representative ICP traces from rats with i.c.v. delivery of Ex4, Ex9-39, or vehicle. Traces are shown before and after shift of infusion solution (marked with a grey line). **E** Summarized changes in the final 15 min ICP measurements (marked in (**D**)) compared to own baseline (shown in percentage, $n = 5–6$, with one outlier removed from the control group and one removed from the Ex9-39 group)). Results are shown as mean ± SEM. Statistical significance was evaluated with one-way ANOVA followed by Dunnett's *post-hoc* test. *; $P < 0.05$, *** $P < 0.001$. Non significance is not shown for clarity

experimental groups was 4.9 ± 0.2 mmHg ($n = 16$). Infusion of Ex4 led to a gradual increase in ICP throughout the experimental window (see representative trace in Fig. 2D), which amounted to an Ex4-mediated ICP increase of 11.9 ± 7.7% ($n = 5$, Fig. 2E), which was significantly higher than that obtained from control rats (a decrease in ICP of 5.1 ± 3.6%, $n = 5$, $p < 0.05$, Fig. 2D-E). The ICP of Ex9-39-infused rats showed no significant change (an ICP decline from baseline of 9.1 ± 1.4%, $n = 6$) compared to control rats ($p = 0.8$, Fig. 2D-E). These results suggest that the observed acute Ex4-mediated increase in CSF flow can lead to an acute elevation of ICP in these rats.

GLP-1R is expressed at low levels in the choroid plexus

The majority of the CSF is produced by the choroid plexus epithelium residing in the brain ventricles [41]. RNAseq of this tissue has demonstrated transcriptional presence at a low level (0.4 TPM) of the gene encoding the GLP-1R (*Glp1r*) [20]. To obtain a visual map of the choroid plexus *Glp1r* transcript expression, we performed RNAscope with the Rn-*Glp1r* RNAscope probe targeting the mRNA encoding GLP-1R. Imaging of excised choroid plexus demonstrated high transcript abundance of the gene encoding the Na^+/K^+-ATPase, α1 subunit (*Atp1a1*), but low transcript abundance of *Glp1r* in a limited number of cells in the choroid plexus of the fourth ventricle (Fig. 3A-C) with an apparently sparser signal in the lateral choroid plexus (near limit of detection, Additional File 1, Figure S1A). These images indicate that the *Glp1r* transcript is indeed detected in the choroid plexus, although at low levels.

To determine if GLP-1R is detected at the protein level in the choroid plexus, we performed western blot analysis of choroid plexus acutely excised from the rat brain. Choroid plexus of both the lateral and fourth ventricles demonstrated presence of GLP-1R (Fig. 3D and Additional File 1, Figure S1B). To confirm GLP-1R protein expression in the choroid plexus, we, in addition, employed the cre-based *Glp1r*-tdTomato reporter mouse line. This line expresses red fluorescent protein under a constitutively active promoter in cells that express the GLP-1R,

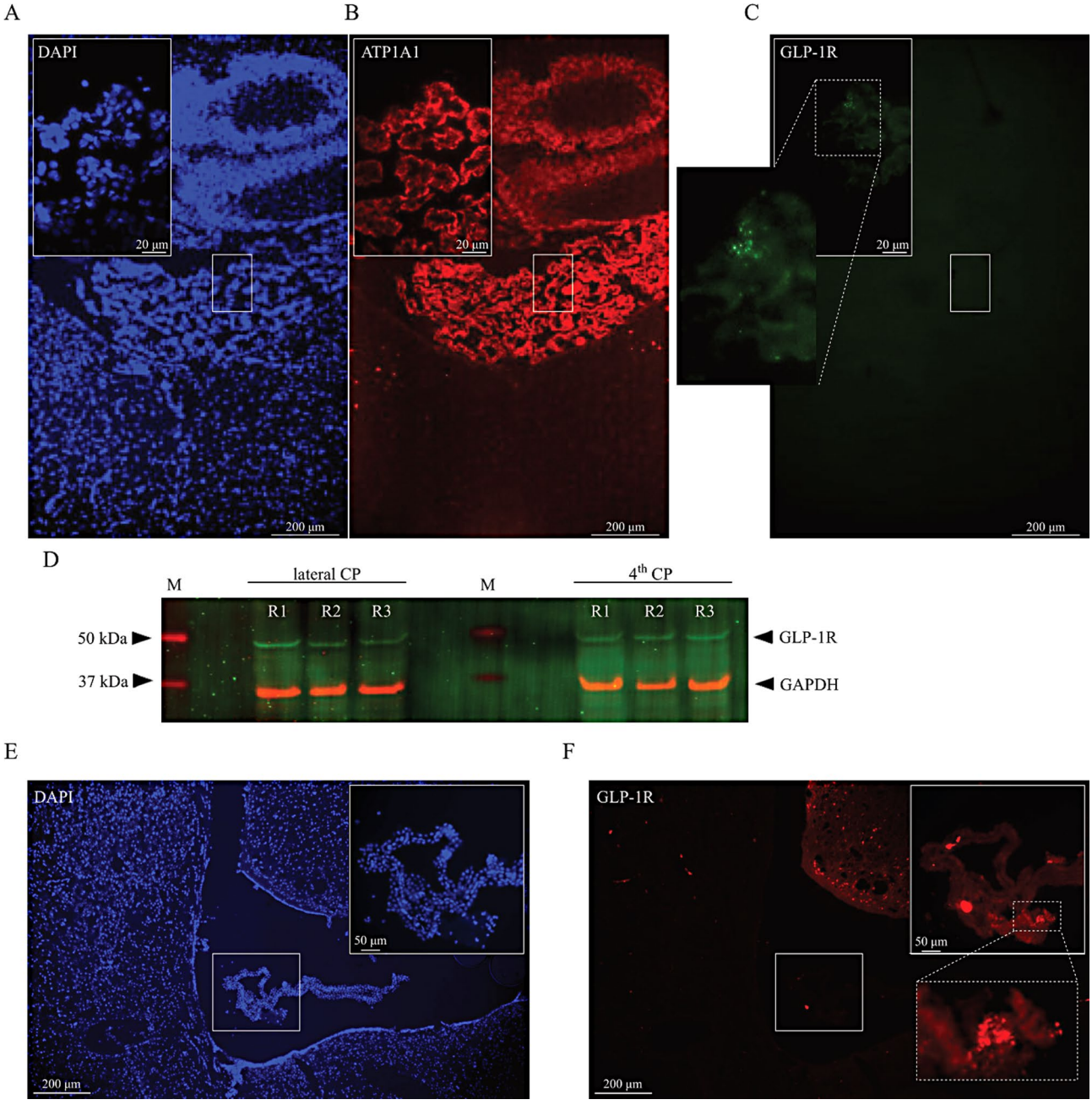

Fig. 3 GLP-1R expression in rat choroid plexus. **A** DAPI staining of choroid plexus (from the fourth ventricle) with the insert representing increased magnification of the area marked with a white box. **B** Representative RNAscope image illustrating mRNA expression of the Na^+/K^+-ATPase (*Atp1a1)* in the choroid plexus of the fourth ventricle with the insert representing increased magnification of the area marked with a white box. **C** Representative RNAscope image illustrating mRNA expression of GLP-1R (*Glp1r*) in the choroid plexus of the fourth ventricle with the insert representing increased magnification of the area marked with a white box. Data in **A**-**C** are from $n = 3$ rats with multiple images obtained in each. **D** Western blot of choroid plexuses (CP, from lateral and fourth ventricles) stained for GLP-1R (green) with GAPDH (red) as a loading control, $n = 3$. **E-F** Representative images of choroid plexus from the fourth ventricle in brain sections obtained from *Glp1r*-tdTomato reporter mice stained with DAPI (**E**) or imaged for the inherent fluorescence (**F**), with the insert representing increased magnification of the area marked with a white box, $n = 3$ mice with multiple images obtained in each

allowing detection even in areas with low GLP-1R expression [18], thus indicating protein expression in a given cell type. Fluorescent images of brain sections obtained from these mice demonstrate a weak, but detectable, signal in the choroid plexus epithelium (Fig. 3E-F).

GLP-1R activation modulates the choroid plexus transporter activity

To reveal the molecular coupling between GLP-1R modulation and the altered CSF secretion rate, we determined the choroid plexus transport activity of the

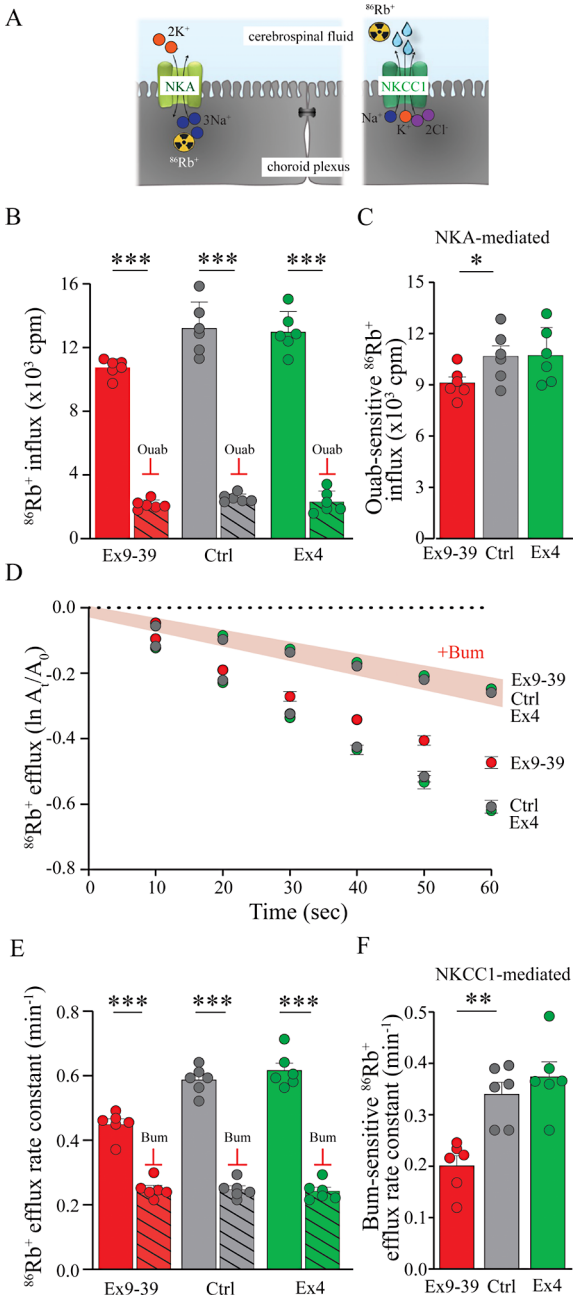

Fig. 4 GLP-1R inhibition reduces choroid plexus transport activity. **A** Schematic representation of the $^{86}Rb^+$ isotope flux assays with uptake on the left panel and efflux on the right panel. **B** $^{86}Rb^+$ influx into acutely excised choroid plexus in the presence and absence of ouabain (Ouab), following pretreatment with Ex9-39, Ex4, or vehicle, $n = 6$ of each. **C** The ouabain-sensitive fraction, representing the Na^+/K^+-ATPase-mediated $^{86}Rb^+$ influx in each choroid plexus, in control conditions and in the presence of Ex9-39 and Ex4, $n = 6$. **D** Efflux of $^{86}Rb^+$ from choroid plexus as a function of time in control settings and following pretreatment with Ex9-39 or Ex4 in the absence or presence of bumetanide (Bum), $n = 6$ of each. The y-axis is the natural logarithm of the remaining $^{86}Rb^+$ in the choroid plexus at time t (A_t), divided by the amount at time 0 (A_0). **E** The efflux rate constant of $^{86}Rb^+$ in choroid plexus in control conditions and after pretreatment with Ex9-39 or Ex4 (linear regression on data from D), $n = 6$. **F** NKCC1-mediated $^{86}Rb^+$ efflux rate constants in control settings and after pretreatment with Ex9-39 or Ex4, $n = 6$. Cpm: counts per minute. The results are presented as mean ± SEM. Statistical significance was evaluated with one-way ANOVA followed by Sidak's *post-hoc* test (**B** and **E**) or Dunnett's *post-hoc* test (**C** and **F**). $^*P < 0.05$, $^{**}P < 0.01$, $^{***}P < 0.001$, Non significance is not shown for clarity

Na^+/K^+-ATPase and the $Na^+,K^+,2Cl^-$ cotransporter 1 (NKCC1) in the presence of GLP-1R-modulating drugs. These transporters are highly expressed in the choroid plexus [20] and are key contributors to CSF secretion [36, 42]. Acutely excised choroid plexus was exposed to Ex4 or Ex9-39 for 10 min prior to initiation of the isotope flux assays based on the K^+ congener $^{86}Rb^+$, which readily replaces K^+ in the transport cycle of both the Na^+/K^+-ATPase and NKCC1 (Fig. 4A). The Na^+/K^+-ATPase activity was determined as a $^{86}Rb^+$ influx assay in the absence and presence of the Na^+/K^+-ATPase inhibitor ouabain (Fig. 4B), and the ouabain-sensitive fraction employed to represent the Na^+/K^+-ATPase activity. Ex9-39 exposure reduced the Na^+/K^+-ATPase activity by ~20% ($8.61 \pm 0.22 \times 10^3$ cpm with Ex9-39 vs. $10.7 \pm 0.6 \times 10^3$ cpm in control, $n = 6$, $p < 0.05$), whereas Ex4 exposure did not alter the Na^+/K^+-ATPase activity ($10.7 \pm 0.7 \times 10^3$ cpm, $n = 6$, $p = 0.52$, Fig. 4C). The NKCC1 activity was determined with an isotope efflux assay following pre-equilibration of $^{86}Rb^+$ in excised choroid plexus, and measured as a function of time in the absence or presence of the NKCC1 inhibitor bumetanide. Figure 4D illustrates the $^{86}Rb^+$ efflux from lateral choroid plexus as a function of time in the presence or absence of Ex4 and Ex9-39 with and without the NKCC1 inhibitor bumetanide and Fig. 4E shows the respective $^{86}Rb^+$ efflux rate constants for each condition. The NKCC1-mediated activity was obtained from the bumetanide-sensitive fraction of the $^{86}Rb^+$ efflux rate. Ex9-39 exposure reduced the NKCC1 activity by ~40% (0.20 ± 0.02 min^{-1} with Ex9-39 vs. 0.34 ± 0.02 min^{-1} in control, $n = 6$, $p < 0.01$), whereas Ex4 exposure did not alter the NKCC1 activity (0.37 ± 0.03, min^{-1}, $n = 6$, $p = 0.59$), Fig. 4F. Taken together, our data suggest that the GLP-1R antagonist Ex9-39 may act directly on the choroid plexus to decrease the activity of both NKCC1 and Na^+/K^+-ATPase.

PKA Inhibition reduces CSF secretion

GLP-1R couples to the G protein of the G_s type, which activates adenylate cyclase to generate cAMP, ultimately leading to protein kinase A (PKA) activation [43, 44]. A GLP-1R antagonist is thus predicted to reduce choroid plexus-mediated CSF secretion through a reduction in a PKA signalling pathway. To mimic such a PKA-inhibiting effect on the choroid plexus, we determined CSF secretion rates upon inhibition of the cAMP/PKA signal cascade. We here employed the ventriculo-cisternal perfusion assay [37, 45], which uses lateral ventricular infusion of equi-osmolar, heated, and gas-equilibrated aCSF containing fluorescent dextran with subsequent

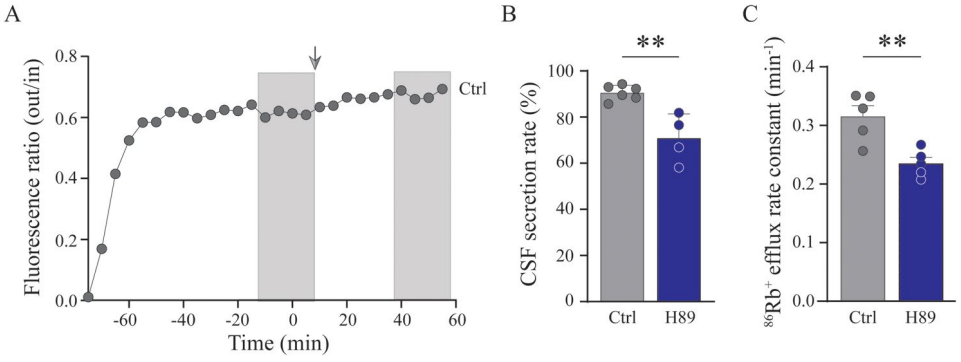

Fig. 5 PKA inhibition lowers CSF secretion and K^+ efflux from the choroid plexus. **A** Representative trace of fluorescent dye dilution over the course of a ventriculo-cisternal perfusion assay in a control rat. The first grey box indicates the values employed as control rate and the second those employed to obtain the percentage change in CSF secretion rate. **B** Summarized CSF secretion rates shown as percentage of own control after infusion with vehicle (control; Ctrl) or the PKA inhibitor H89, $n = 4$–6. **C** Efflux rate constant for $^{86}Rb^+$ from acutely excised choroid plexuses treated with vehicle (Ctrl) or H89, $n = 5$ of each. Results are shown as mean ± SEM. Statistical significance was evaluated with Student's unpaired t-test. **; $P < 0.01$

collection from a cisterna magna puncture. Fluorescence dilution upon passage through the ventricular system (Fig. 5A) is due to de novo secretion of CSF, allowing calculation of the inhibitor-induced changes in the CSF secretion rate. Upon stabilization of the fluorescent outflow, the infusion solution was replaced with one containing either vehicle (time control) or the PKA inhibitor H89 (250 µM). The internal time control demonstrated a final CSF secretion rate of 91 ± 1% of the control value obtained prior to solution shift, $n = 6$, whereas replacement of the aCSF vehicle infusion solution with one containing H89 reduced the CSF secretion rate to 71 ± 5% of control, $n = 4$, $P < 0.01$, Fig. 5B. Determination of efflux of the K^+ congener $^{86}Rb^+$, preloaded into acutely excised ex vivo choroid plexus, revealed a 25% reduction of the K^+ efflux across the luminal membrane of the choroid plexus with PKA inhibition (0.32 ± 0.02 min^{-1} in control vs. 0.24 ± 0.01 min^{-1} with H89, $n = 5$ of each, $P < 0.01$, Fig. 5C), suggesting a reduction in the transport activity of NKCC1 and/or other K^+ channels or transporters upon PKA inhibition.

Discussion

We here demonstrate that modulation of the GLP-1R by an agonist or an antagonist changes the rate of CSF secretion, in part via its action on choroid plexus transporters in experimental rats. GLP-1 is generally associated with satiety and food intake, but can also modulate systemic fluid homeostasis via its receptor-mediated action on electrolyte transport mechanisms in other epithelia such as those of the small intestine and the kidney [10, 12–14]. Neither the GLP-1R agonist Ex4, nor the antagonist Ex9-39 modulated the CSF secretion rate when delivered systemically (i.p.) in the here employed dosages, whereas central delivery (i.c.v.) caused a 38% Ex4-mediated increase in the CSF secretion rate and a 60% Ex9-39-mediated decrease in CSF secretion. Of note, the CSF secretion assays employed here and elsewhere do not address the origin of the CSF. The CSF flow, as here quantified, is thus employed as a proxy for CSF secretion, and has repeatedly been demonstrated to be affected similarly to CSF secretion rates obtained by the ventriculo-cisternal perfusion assay by different modulators (activator/inhibitors) [36, 37, 46, 47]. Nevertheless, we cannot exclude that potential Ex-mediated changes in blood pressure and arterial pulsations could affect our result. We observed no prolonged (24 h) effect on overall brain water content following either of the treatments, and no significant short term effect on ICP by the Ex9-39-mediated reduction in CSF secretion, which may originate from the brain compliancy. The Ex4-mediated increase in CSF secretion resulted in an acute, but minor, increase in ICP of approximately 10%. An earlier study, which did not quantify in vivo CSF secretion, detected a swift (< 5 min) decrease in rat ICP following systemic Ex4 exposure, both in healthy rats and in rats with experimentally-induced hydrocephalus [21]. While we cannot explain the discrepancy, the previous study mostly employed i) higher concentrations of Ex4 (5–20 µg/kg) than used here (0.2 µg/kg), subcutaneous delivery of Ex4 as their peripheral route, whereas we here employed i.p. delivery, iii) telemetric ICP probes, whereas we here determined ICP epidurally in anaesthetized rats during i.c.v. infusion of Ex4 or Ex9-39, and iv) their use of midazolam as anaesthesia, which has been reported to modulate ICP and perfusion pressure in patients [48]. Either of these differences alone or together could promote an Ex4-mediated reduction in ICP as observed in [21]. The high concentrations and subcutaneous delivery route of Ex4 could potentially influence systemic physiological parameters indirectly lowering ICP in a manner distinct from its direct effect on the choroid plexus GLP-1R-mediated increase in CSF secretion. With the abundant GLP-1R expression throughout the brain, taken together

with its reported effect on energy homeostasis, appetite and weight control, and neuroprotection [15], GLP-1R modulation may alter brain function and associated CSF dynamics in manners distinct from those originating in choroid plexus.

The GLP-1R is expressed at low levels in the choroid plexus, as detected at the transcript level with RNAseq in rats [20] and qPCR in humans [21], and here confirmed with RNAscope. These data demonstrated expression of GLP-1R in choroid plexus near the limit of detection, with a striking difference to the well-established abundant Na^+/K^+-ATPase expression. GLP-1R protein expression was verified with Western blotting in rat choroid plexus (albeit with much lower signal than in hypothalamus, Additional File 1, Figure S1C) and confirmed with weak fluorescent signal in a limited number of choroid plexus epithelial cells in the GLP-1R reporter mouse. The observation of a weak fluorescent signal in the choroid plexus obtained from the GLP-1R reporter mice may reflect rapid breakdown of the tdtomato protein within the tissue. A previous study has assigned the receptor to the luminal face of epithelial cells of the choroid plexus in post-mortem human tissue [21]. The GLP-1R is a class B G protein-coupled receptor that predominantly couples to G_s, thereby activating adenylate cyclase and promoting generation of cAMP [43, 44]. As a result, GLP-1R activation in cultured choroid plexus epithelial cells increases cAMP production [21]. Elevated cAMP facilitates the transport of chloride (one of the key electrolytes driving CSF secretion [42, 49]) from the vasculature, across the choroid plexus, to the CSF [50], which aligns with cAMP-mediated increased CSF production in dogs [45]. Inhibition of cAMP production thus ought to reduce CSF secretion and transport activity across choroid plexus. Accordingly, we demonstrate that direct inhibition of the cAMP-dependent protein kinase PKA lowers CSF secretion, in part via reduced NKCC1 activity. Taken together, these data suggest a GLP-1R induced cAMP – and thus possibly GLP-1R – mediated increase in CSF secretion, and a reduction thereof upon inhibition of the receptor or its downstream signalling cascade. The transport proteins NKCC1 and the Na^+/K^+-ATPase reside on the luminal membrane of the choroid plexus and are amongst the key contributors to CSF secretion by this tissue [36, 37]. These transporters both displayed reduced activity upon inhibition of the GLP-1R with Ex9-39 in acutely excised rat choroid plexus, which supports luminal expression of GLP-1R [21]. This GLP-1R-mediated modulation of transport activity likely represents the molecular coupling between GLP-1R inhibition and the observed Ex9-39-induced reduction in CSF secretion, via reduced cAMP-dependent protein kinase A-mediated phosphorylation of NKCC1 and the Na^+/K^+-ATPase, and thus lowered activity of these proteins [51–53]. Ex4-induced modulation of GLP-1R in the excised choroid plexus did not significantly increase the transport activity of the two tested transporters, suggesting a satiated level of cAMP with excision of the choroid plexus and/or that the Ex4-mediated increase in in vivo CSF secretion arises from other contributing (bicarbonate) transporters, via endogenous factors in the native CSF, and/or via modulation of various central physiological parameters, possibly via the high levels of GLP-1R expression in the hypothalamus, that may indirectly affect the CSF secretion rate.

Modulation of the GLP-1R could potentially be employed as a pharmacological approach to manage elevated ICP in patients with ICP-related conditions [54]. In addition to GLP-1R-mediated effects on ICP itself, the weight loss associated with prolonged GLP-1R agonist intake [55, 56] is predicted to contribute to reduced ICP in obese idiopathic intracranial hypertension (IIH) patients, in whom weight loss represents a definite intervention to improve symptoms [57]. A recent small clinical trial employing the GLP-1R agonist Exenatide, which has the same amino acid sequence as Ex4, demonstrated promising early results (ICP reductions of 1–3 mmHg) in IIH patients [27]. Some of the monitored values (i.e., headache days and visual parameters) varied between the control and treatment groups prior to treatment initiation, which may complicate final conclusions until a larger follow-up trial is conducted. It remains to be delineated how GLP-1R may modulate ICP directly and indirectly, whether it compromises the blood-CSF barrier or affects CSF reabsorption, if species-specific differences may occur, and if off-target effects may contribute to modulation of the CSF dynamics. However, another GLP-1 receptor agonist, semaglutide, has been associated with increased risk of non-arteritic anterior ischemic optic neuropathy (NAION) [58], which can lead to vision loss due to optic nerve damage. We here demonstrate increased ICP following central exposure to Ex4. As such ICP increase is linked to papilledema and optic nerve damage [59, 60], it is possible that semaglutide-mediated ICP elevation may exacerbate ischemic conditions in the optic nerve and contribute to the development of NAION. Although we did not observe increased ICP with systemic delivery of Ex4, this potential side effect and its underlying etiology warrant further investigation, given the growing use of semaglutide for diabetes and obesity.

In conclusion, we here demonstrate that choroid plexus GLP-1R activation, possibly via its concomitant cAMP elevation, increases CSF secretion and ICP in healthy rats. Receptor inhibition, conversely, lowers CSF secretion analogously to the decrease in secretion observed with inhibition of the cAMP/PKA signalling cascade, in part via its inhibitory effect on choroid plexus transporters. Future research using GLP-1R antagonists to reduce

ICP in pathologies with raised ICP will reveal its potential as a pharmacological tool to manage ICP. However, such approach is presently challenged by the required central delivery route for an effect of Ex9-39 on CSF dynamics. Future research on Ex9-39 with improved brain penetration is thus warranted.

Supplementary Information

The online version contains supplementary material available at https://doi.org/10.1186/s12987-025-00652-x.

Supplementary Material 1: Additional File 1: RNAscope and Western blot

Acknowledgements
We are grateful for technical assistance from Trine Lind Devantier, Rikke Lundorf, and Adrian Dragen.

Author contributions
NM, MMR designed the research study; JJH, MFR, DBA supplied critical resources and technical/experimental knowledge; MNJ, IMEI, JHW, DBJ, IMEI, TLTB, MMR carried out the experiments; MNJ, IMEI, JHW, DBJ, IMEI, TLTB, MFR, DBA, MMR analyzed the data; MNJ and NM drafted the manuscript, and all authors revised and approved the final version.

Funding
Open access funding provided by Copenhagen University.
This project was funded by the Lundbeck Foundation (R276-2018-403 to NM, R303-2018-3005 to TLTB), the Novo Nordic Foundation (tandem grant NNF17OC0024718 to NM), and the Carlsberg Foundation (CF19-0056 to NM).

Data availability
The datasets used in the current study are available from the corresponding author on reasonable request.

Declarations

Ethical approval
Animal experiments were in compliance with the European Community Council Directive 2010/63/EU on the Protection of Animals used for Scientific Purposes. It was approved by the Danish Animal Experiments Inspectorate with permission no. 2021-15-0201-00867 and 2018-15-0201-01397).

Consent for publication
Not applicable.

Competing interests
The authors declare no competing interests.

Received: 10 January 2025 / Accepted: 6 April 2025
Published online: 24 April 2025

References

1. Damkier HH, Brown PD, Praetorius J. Cerebrospinal fluid secretion by the choroid plexus. Physiol Rev. 2013;93:1847–92.
2. Ziebell M, Wetterslev J, Tisell M, Gluud C, Juhler M. Flow-regulated versus differential pressure-regulated shunt valves for adult patients with normal pressure hydrocephalus. Cochrane Database Syst Rev. 2013;5:CD009706.
3. Smith M, Reddy U, Robba C, Sharma D, Citerio G. Acute ischaemic stroke: challenges for the intensivist. Intensive Care Med. 2019;45:1177–89.
4. Holst JJ. Discovery of the GI effects of GLP-1: an historical perspective. Dig Dis Sci. 2022;67:2716–20.
5. Wettergren A, Schjoldager B, Mortensen PE, Myhre J, Christiansen J, Holst JJ. Truncated GLP-1 (proglucagon 78-107-amide) inhibits gastric and pancreatic functions in man. Dig Dis Sci. 1993;38:665–73.
6. Alhadeff AL, Grill HJ. Hindbrain nucleus tractus solitarius glucagon-like peptide-1 receptor signaling reduces appetitive and motivational aspects of feeding. Am J Physiol Regul Integr Comp Physiol. 2014;307:R465–70.
7. Astrup A, Rössner S, Van Gaal L, Rissanen A, Niskanen L, Al Hakim M, Madsen J, Rasmussen MF, Lean ME. Effects of liraglutide in the treatment of obesity: a randomised, double-blind, placebo-controlled study. Lancet. 2009;374:1606–16.
8. Flint A, Raben A, Astrup A, Holst JJ. Glucagon-like peptide 1 promotes satiety and suppresses energy intake in humans. J Clin Invest. 1998;101:515–20.
9. Larsen PJ, Tang-Christensen M, Holst JJ, Orskov C. Distribution of glucagon-like peptide-1 and other preproglucagon-derived peptides in the rat hypothalamus and brainstem. Neuroscience. 1997;77:257–70.
10. Tang-Christensen M, Larsen PJ, Göke R, Fink-Jensen A, Jessop DS, Møller M, Sheikh SP. Central administration of GLP-1-(7–36) amide inhibits food and water intake in rats. Am J Physiol. 1996;271:R848–56.
11. Turton MD, O'Shea D, Gunn I, Beak SA, Edwards CM, Meeran K, Choi SJ, Taylor GM, Heath MM, Lambert PD, Wilding JP, Smith DM, Ghatei MA, Herbert J, Bloom SR. A role for glucagon-like peptide-1 in the central regulation of feeding. Nature. 1996;379:69–72.
12. Carraro-Lacroix LR, Malnic G, Girardi AC. Regulation of Na+/H + exchanger NHE3 by glucagon-like peptide 1 receptor agonist exendin-4 in renal proximal tubule cells. Am J Physiol Ren Physiol. 2009;297:F1647–55.
13. Muskiet MH, Smits MM, Morsink LM, Diamant M. The gut-renal axis: do incretin-based agents confer renoprotection in diabetes? Nat Rev Nephrol. 2014;10:88–103.
14. Muskiet MHA, Tonneijck L, Smits MM, van Baar MJB, Kramer MHH, Hoorn EJ, Joles JA, van Raalte DH. GLP-1 and the kidney: from physiology to Pharmacology and outcomes in diabetes. Nat Rev Nephrol. 2017;13:605–28.
15. Candeias EM, Sebastião IC, Cardoso SM, Correia SC, Carvalho CI, Plácido AI, Santos MS, Oliveira CR, Moreira PI, Duarte AI. Gut-brain connection: the neuroprotective effects of the anti-diabetic drug liraglutide. World J Diabetes. 2015;6:807–27.
16. Drucker DJ, Holst JJ. The expanding incretin universe: from basic biology to clinical translation. Diabetologia. 2023;66:1765–79.
17. Winther JB, Holst JJ. Glucagon agonism in the treatment of metabolic diseases including type 2 diabetes mellitus and obesity. Diabetes Obes Metab. 2024;26:3501–12.
18. Hullon D, Subeh GK, Volkova Y, Janiec K, Trach A, Mnevets R. The role of glucagon-like peptide-1 receptor (GLP-1R) agonists in enhancing endothelial function: a potential avenue for improving heart failure with preserved ejection fraction (HFpEF). Cardiovasc Diabetol. 2025;24:70.
19. Candeias EM, Sebastiao IC, Cardoso SM, Correia SC, Carvalho CI, Placido AI, Santos MS, Oliveira CR, Moreira PI, Duarte AI. Gut-brain connection: the neuroprotective effects of the anti-diabetic drug liraglutide. World J Diabetes. 2015;6:807–27.
20. Andreassen SN, Toft-Bertelsen TL, Wardman JH, Villadsen R, MacAulay N. Transcriptional profiling of transport mechanisms and regulatory pathways in rat choroid plexus. Fluids Barriers CNS. 2022;19:44.
21. Botfield HF, Uldall MS, Westgate CSJ, Mitchell JL, Hagen SM, Gonzalez AM, Hodson DJ, Jensen RH, Sinclair AJ. A glucagon-like peptide-1 receptor agonist reduces intracranial pressure in a rat model of hydrocephalus. Sci Transl Med. 2017;9(404):eaan0972.
22. Andersen DB, Grunddal KV, Pedersen J, Kuhre RE, Lund ML, Holst JJ, et al. Using a reporter mouse to map known and novel sites of GLP-1 receptor expression in peripheral tissues of male mice. Endocrinology. 2021;162(3):bqaa246.
23. Gea LP, da Rosa ED, Panizzutti BS, de Aguiar EZ, de Oliveira LF, Ferrari P, Piato A, Gomez R, Colombo R, Rosa AR. Reduction of hippocampal IL-6 levels in LPS-injected rats following acute exendin-4 treatment. Naunyn Schmiedebergs Arch Pharmacol. 2020;393:1303–11.
24. Hayes MR, Skibicka KP, Grill HJ. Caudal brainstem processing is sufficient for behavioral, sympathetic, and parasympathetic responses driven by peripheral and hindbrain glucagon-like-peptide-1 receptor stimulation. Endocrinology. 2008;149:4059–68.
25. Darsalia V, Hua S, Larsson M, Mallard C, Nathanson D, Nystrom T, Sjoholm A, Johansson ME, Patrone C. Exendin-4 reduces ischemic brain injury in normal and aged type 2 diabetic mice and promotes microglial M2 polarization. PLoS ONE. 2014;9:e103114.
26. Augestad IL, Dekens D, Karampatsi D, Elabi O, Zabala A, Pintana H, Larsson M, Nystrom T, Paul G, Darsalia V, Patrone C. Normalisation of glucose metabolism by exendin-4 in the chronic phase after stroke promotes functional recovery in male diabetic mice. Br J Pharmacol. 2022;179:677–94.

27. Mitchell JL, Lyons HS, Walker JK, Yiangou A, Grech O, Alimajstorovic Z, Greig NH, Li Y, Tsermoulas G, Brock K, Mollan SP, Sinclair AJ. The effect of GLP-1RA exenatide on idiopathic intracranial hypertension: a randomized clinical trial. Brain. 2023;146:1821–30.
28. Dickson SL, Shirazi RH, Hansson C, Bergquist F, Nissbrandt H, Skibicka KP. The glucagon-like peptide 1 (GLP-1) analogue, exendin-4, decreases the rewarding value of food: a new role for mesolimbic GLP-1 receptors. J Neurosci. 2012;32:4812–20.
29. Ahren B. Contribution of GIP and GLP-1 to the insulin response to oral administration of glucose in female mice. Biomedicines. 2023;11(2):591.
30. Sorensen H, Winzell MS, Brand CL, Fosgerau K, Gelling RW, Nishimura E, Ahren B. Glucagon receptor knockout mice display increased insulin sensitivity and impaired beta-cell function. Diabetes. 2006;55:3463–9.
31. Hansen LS, Sparre-Ulrich AH, Christensen M, Knop FK, Hartmann B, Holst JJ, Rosenkilde MM. N-terminally and C-terminally truncated forms of glucose-dependent insulinotropic polypeptide are high-affinity competitive antagonists of the human GIP receptor. Br J Pharmacol. 2016;173:826–38.
32. Kissow H, Hartmann B, Holst JJ, Viby NE, Hansen LS, Rosenkilde MM, Hare KJ, Poulsen SS. Glucagon-like peptide-1 (GLP-1) receptor agonism or DPP-4 Inhibition does not accelerate neoplasia in carcinogen treated mice. Regul Pept. 2012;179:91–100.
33. Steffensen AB, Edelbo BL, Barbuskaite D, Andreassen SN, Olsen MH, Møller K, MacAulay N. Nocturnal increase in cerebrospinal fluid secretion as a regulator of intracranial pressure. Fluids Barriers CNS. 2023;20:49.
34. Craig CM, Liu LF, Nguyen T, Price C, Bingham J, McLaughlin TL. Efficacy and pharmacokinetics of subcutaneous Exendin (9–39) in patients with post-bariatric hypoglycaemia. Diabetes Obes Metab. 2018;20:352–61.
35. Parkes D, Jodka C, Smith P, Nayak S, Rinehart L, Gingerich R, Chen K, Young A. Pharmacokinetic actions of exendin-4 in the rat: comparison with glucagon-like peptide-1. Drug Develop Res. 2001;53:260–67.
36. Oernbo EK, Steffensen AB, Razzaghi Khamesi P, Toft-Bertelsen TL, Barbuskaite D, Vilhardt F, Gerkau NJ, Tritsaris K, Simonsen AH, Lolansen SD, Andreassen SN, Hasselbalch SG, Zeuthen T, Rose CR, Kurtcuoglu V, MacAulay N. Membrane transporters control cerebrospinal fluid formation independently of conventional osmosis to modulate intracranial pressure. Fluids Barriers CNS. 2022;19:65.
37. Steffensen AB, Oernbo EK, Stoica A, Gerkau NJ, Barbuskaite D, Tritsaris K, Rose CR, MacAulay N. Cotransporter-mediated water transport underlying cerebrospinal fluid formation. Nat Commun. 2018;9:2167.
38. Barragan JM, Rodriguez RE, Eng J, Blazquez E. Interactions of exendin-(9–39) with the effects of glucagon-like peptide-1-(7–36) amide and of exendin-4 on arterial blood pressure and heart rate in rats. Regul Pept. 1996;67:63–8.
39. Roan JN, Hsu CH, Fang SY, Tsai HW, Luo CY, Huang CC, Lam CF. Exendin-4 improves cardiovascular function and survival in flow-induced pulmonary hypertension. J Thorac Cardiovasc Surg. 2018;155:1661–69. e4.
40. Viby NE, Isidor MS, Buggeskov KB, Poulsen SS, Hansen JB, Kissow H. Glucagon-like peptide-1 (GLP-1) reduces mortality and improves lung function in a model of experimental obstructive lung disease in female mice. Endocrinology. 2013;154:4503–11.
41. MacAulay N, Keep RF, Zeuthen T. Cerebrospinal fluid production by the choroid plexus: a century of barrier research revisited. Fluids Barriers CNS. 2022;19:26.
42. MacAulay N. Molecular mechanisms of brain water transport. Nat Rev Neurosci. 2021;22:326–44.
43. Graaf C, Donnelly D, Wootten D, Lau J, Sexton PM, Miller LJ, Ahn JM, Liao J, Fletcher MM, Yang D, Brown AJ, Zhou C, Deng J, Wang MW. Glucagon-Like Peptide-1 and its class B G Protein-Coupled receptors: A long March to therapeutic successes. Pharmacol Rev. 2016;68:954–1013.
44. Wootten D, Reynolds CA, Smith KJ, Mobarec JC, Koole C, Savage EE, Pabreja K, Simms J, Sridhar R, Furness SGB, Liu M, Thompson PE, Miller LJ, Christopoulos A, Sexton PM. The extracellular surface of the GLP-1 receptor is a molecular trigger for biased agonism. Cell. 2016;165:1632–43.
45. Epstein MH, Feldman AM, Brusilow SW. Cerebrospinal fluid production: stimulation by cholera toxin. Science. 1977;196:1012–3.
46. Toft-Bertelsen TL, Barbuskaite D, Heerfordt EK, Lolansen SD, Andreassen SN, Rostgaard N, Olsen MH, Norager NH, Capion T, Rath MF, Juhler M, MacAulay N. Lysophosphatidic acid as a CSF lipid in posthemorrhagic hydrocephalus that drives CSF accumulation via TRPV4-induced hyperactivation of NKCC1. Fluids Barriers CNS. 2022;19:69.
47. Wardman JH, Jensen MN, Andreassen SN, Styrishave B, Wilhjelm JE, Sinclair AJ, MacAulay N. Modelling idiopathic intracranial hypertension in rats: contributions of high fat diet and testosterone to intracranial pressure and cerebrospinal fluid production. Fluids Barriers CNS. 2023;20:44.
48. Papazian L, Albanese J, Thirion X, Perrin G, Durbec O, Martin C. Effect of bolus doses of Midazolam on intracranial pressure and cerebral perfusion pressure in patients with severe head injury. Br J Anaesth. 1993;71:267–71.
49. Maren TH, Broder LE. The role of carbonic anhydrase in anion secretion into cerebrospinal fluid. J Pharmacol Exp Ther. 1970;172:197–202.
50. Deng QS, Johanson CE. Cyclic AMP alteration of chloride transport into the choroid plexus-cerebrospinal fluid system. Neurosci Lett. 1992;143:146–50.
51. Flemmer AW, Monette MY, Djurisic M, Dowd B, Darman R, Gimenez I, Forbush B. Phosphorylation state of the Na+-K+-Cl- cotransporter (NKCC1) in the gills of Atlantic killifish (Fundulus heteroclitus) during acclimation to water of varying salinity. J Exp Biol. 2010;213:1558–66.
52. Kurihara K, Nakanishi N, Moore-Hoon ML, Turner RJ. Phosphorylation of the salivary Na(+)-K(+)-2Cl(-) cotransporter. Am J Physiol Cell Physiol. 2002;282:C817–23.
53. Liu L, Bulla LA. Jr. Cell death signaling in Anopheles Gambiae initiated by Bacillus Thuringiensis Cry4B toxin involves Na(+)/K(+) ATPase. Exp Biol Med. 2023;248:1191–205.
54. Yiangou A, Mollan SP, Sinclair AJ. Idiopathic intracranial hypertension: a step change in Understanding the disease mechanisms. Nat Rev Neurol. 2023;19:769–85.
55. Haddad F, Dokmak G, Bader M, Karaman R. A comprehensive review on weight loss associated with Anti-Diabetic medications. Life (Basel). 2023;13(4):1012.
56. Sun F, Chai S, Li L, Yu K, Yang Z, Wu S, Zhang Y, Ji L, Zhan S. Effects of glucagon-like peptide-1 receptor agonists on weight loss in patients with type 2 diabetes: a systematic review and network meta-analysis. J Diabetes Res. 2015; 157201.
57. Mollan SP, Mitchell JL, Ottridge RS, Aguiar M, Yiangou A, Alimajstorovic Z, Cartwright DM, Grech O, Lavery GG, Westgate CSJ, Vijay V, Scotton W, Wakerley BR, Matthews TD, Ansons A, Hickman SJ, Benzimra J, Rick C, Singhal R, Tahrani AA, Brock K, Frew E, Sinclair AJ. Effectiveness of bariatric surgery vs community weight management intervention for the treatment of idiopathic intracranial hypertension: A randomized clinical trial. JAMA Neurol. 2021;78:678–86.
58. Hathaway JT, Shah MP, Hathaway DB, Zekavat SM, Krasniqi D, Gittinger JW Jr., Cestari D, Mallery R, Abbasi B, Bouffard M, Chwalisz BK, Estrela T, Rizzo JF. 3rd. Risk of nonarteritic anterior ischemic optic neuropathy in patients prescribed semaglutide. JAMA Ophthalmol. 2024;142:732–39.
59. Xie JS, Donaldson L, Margolin E, Papilledema. A review of etiology, pathophysiology, diagnosis, and management. Surv Ophthalmol. 2022;67:1135–59.
60. Hayreh SS. Pathogenesis of optic disc edema in Raised intracranial pressure. Prog Retin Eye Res. 2016;50:108–44.

Publisher's note